



HAL
open science

How to produce high specific activity tin-117 m using alpha particle beam

C. Duchemin, M. Essayan, Arnaud Guertin, Ferid Haddad, Nathalie Michel,
Vincent Métivier

► **To cite this version:**

C. Duchemin, M. Essayan, Arnaud Guertin, Ferid Haddad, Nathalie Michel, et al.. How to produce high specific activity tin-117 m using alpha particle beam. *Applied Radiation and Isotopes*, 2016, 115, pp.113-124. 10.1016/j.apradiso.2016.06.016 . hal-02912142

HAL Id: hal-02912142

<https://hal.science/hal-02912142v1>

Submitted on 15 Jan 2021

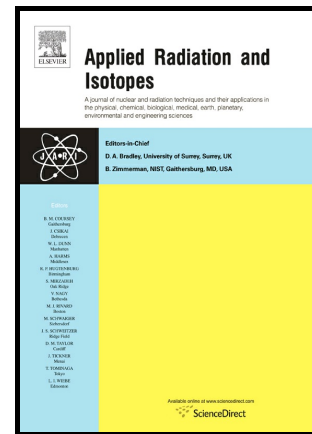
HAL is a multi-disciplinary open access archive for the deposit and dissemination of scientific research documents, whether they are published or not. The documents may come from teaching and research institutions in France or abroad, or from public or private research centers.

L'archive ouverte pluridisciplinaire **HAL**, est destinée au dépôt et à la diffusion de documents scientifiques de niveau recherche, publiés ou non, émanant des établissements d'enseignement et de recherche français ou étrangers, des laboratoires publics ou privés.

Author's Accepted Manuscript

How to produce high specific activity tin-117m using alpha particle beam

C. Duchemin, M. Essayan, A. Guertin, F. Haddad, N. Michel, V. Métivier



PII: S0969-8043(16)30273-1

DOI: <http://dx.doi.org/10.1016/j.apradiso.2016.06.016>

Reference: ARI7521

To appear in: *Applied Radiation and Isotopes*

Received date: 16 March 2016

Revised date: 15 June 2016

Accepted date: 16 June 2016

Cite this article as: C. Duchemin, M. Essayan, A. Guertin, F. Haddad, N. Miche and V. Métivier, How to produce high specific activity tin-117m using alpha particle beam, *Applied Radiation and Isotopes* <http://dx.doi.org/10.1016/j.apradiso.2016.06.016>

This is a PDF file of an unedited manuscript that has been accepted for publication. As a service to our customers we are providing this early version of the manuscript. The manuscript will undergo copyediting, typesetting, and review of the resulting galley proof before it is published in its final citable form. Please note that during the production process errors may be discovered which could affect the content, and all legal disclaimers that apply to the journal pertain

How to produce high specific activity tin-117m using alpha particle beam.

C. Duchemin^a, M. Essayan^a, A. Guertin^a, F. Haddad^{a,b}, N. Michel^{a,b}, V. Métivier^a

^a*SUBATECH, Ecole des Mines de Nantes, Université de Nantes, CNRS/IN2P3, 44307 Nantes, France*

^b*GIP Arronax, 1 rue Aronnax, 44817 Saint-Herblain, France*

Abstract

HIGHLIGHTS

- Cd-116(α ,3n)Sn-117m.
- High specific activity Sn-117m.
- Theranostic isotope.

ABSTRACT

Tin-117m is an interesting radionuclide for both diagnosis and therapy, thanks to the gamma-ray and electron emissions, respectively, resulting from its decay to tin-117g. The high specific activity of tin-117m is required in many medical applications, and it can be obtained using a high energy alpha particle beam and a cadmium target. The experiments performed at the ARRONAX cyclotron (Nantes, France) using an alpha particle beam delivered at 67.4 MeV provide a measurement of the excitation function of the Cd-nat(α ,x)Sn-117m reaction and the produced contaminants. The Cd-116(α ,3n)Sn-117m production cross section has been deduced from these experimental results using natural cadmium. Both production yield and specific activity as a function of the projectile energy have been calculated. These informations help to optimize the irradiation conditions to produce tin-117m with the required specific activity using particles with a cadmium target.

Email address: Charlotte.Duchemin@subatech.in2p3.fr (C. Duchemin)

Keywords: Tin-117m, cadmium target, ARRONAX cyclotron, specific activity

1. Introduction

1.1. *The medical interest of tin-117m*

It has been demonstrated since long ago, that β - emitters are quite effective to relieve bone metastasis pain; in the 60s for phosphorus-32 (Joshi et al., 1965) and in the 90s for strontium-89 (Porter et al. 1993), samarium-153 (Collins et al., 1993, Resche et al., 1997) and rhenium-186g (Maxon et al., 1991, De Klerk et al., 1997). For these β - emitters, the mean energy (maximum energy) of the emitted electrons varies from one isotope to another, leading to a range in tissues from 0.4 mm to 3 mm (from 2 mm to 8 mm). Since the emitted electrons follow a certain energy distribution, even if these β - emitters show a good vectorization to the bone metastases, there are always electrons irradiating the radiosensitive bone marrow (Srivastava et al., 1998). This can be avoided by using fixed energy electrons from electron conversion emitters. It is then possible, by choosing the right radionuclide, to have a better control of the dose distribution, with a higher dose on painful bone metastases and a lower dose in the bone marrow. An article from 1973 (Yano et al., 1973) presents the interest of tin-117m in medicine from the study of several chelates in rats. The study shows the high uptake of tin-117m in the bones, with a low absorption in the normal tissues. Tin-117m is a conversion electron emitter (129.36 keV (65.7%), 129.36 keV (11.65%) and 151.56 keV (26.5%)) with a half-life of 13.60 (4) days (Kinsey et al., 1996, Ekström and Firestone, 2004). The emitted electrons have a range in water from 0.2 to 0.3 mm, depending on the considered electron. In 1998, results on dosimetric calculations were published, showing a comparison between the dose received by the bones, and that received by the bone marrow in the case of β - emitters and Sn-117m (Srivastava et al., 1998). The results showed that the dose ratio bone/bone marrow is, for Sn-117m, 4.1 times higher than that of Sr-89, which in turn is 2.7 times higher than that of Sm-153 and 1.2 times higher than that of Re-186. The therapeutic advantage of the conversion electrons emitted by tin-117m, compared with β - emitters, has been experimentally shown in 2000 (Bishayee et al., 2000). In addition to conversion electrons, gamma emissions also occur during Sn-117m decay. In particular, it emits a 158 keV gamma ray (branching ration 87%), which is suitable for

SPECT imaging. After decay, the Sn-117m changes into the stable Sn-117g nuclide. Sn-117m can then be used as a theranostic agent (Srivastava, 2014) thanks to the gamma and conversion electron emission. The Clear Vascular Company in Texas (USA) is dedicated to clinical trials with special emphasis on the diagnosis and therapy of vulnerable plaques (Clear Vascular Inc., 2015, Lafont, 2003) and other inflammatory diseases. This company has developed an injectable radiopharmaceutical called "Tin-Annexin", composed by tin-117m chelated to Annexin V using a DOTA chelate. Pre-clinical and clinical trials, using this radiopharmaceutical made of Annexin V labelled with Sn-117m, have led to the diagnosis of vulnerable plaques, showing its therapeutic effects on them (Clear Vascular Inc., 2015).

1.2. The tin-117m production routes

Tin-117m can be produced by the neutron activation of tin-116 or tin-117g in reactors. However, its production requires between 2 and 3 weeks of irradiation, and the final product has a low specific activity of the order of the Ci/g. A specific activity between 100 to 1000 Ci/g could be obtained with the use of an additional step of electromagnetic mass separation (Clear Vascular Inc., 2015). Another way to get high specific activity product is to use charged particles (protons, deuterons or α particles) as projectiles. Two main production routes have been identified for the tin-117m production. The Sb-nat(p,x)Sn-117m reaction has been studied by the Institute for Nuclear Research (Russian Academy of Science, 2015). Data have been published in 2007 by Ermolaev et al. (Ermolaev et al., 2007) and in 2013 by Tákács et al. (Tákács et al., 2013). With this reaction, the expected specific activity is close to 1 kCi/g. Another way is to use α particles as projectiles impinging on a Cd-116 enriched target. Even if there is a limited number of accelerators delivering high energy and high intensity α particle beams, this route is currently used to produce tin-117m for clinical trials. Indeed, due to its half-life of several days, the irradiation can be performed in few facilities whereas the target is sent to a radiopharmaceutical company, before its deliver to treatment centers. Two data sets have been published for this reaction up to 42 MeV. Therefore, there is a lack of data at high energy, which is unfortunate since industrial production uses energies above 42 MeV. One thick target production yield estimation has been made on the energy range of 47-20 MeV, based on Qaim et al. calculations (Qaim and Döhler, 1984), and leads to 150 $\mu\text{Ci}/\mu\text{Ah}$. However, this value can be discussed, since the data from Qaim and Döhler, 1984, are not in agreement with most recent ones found

Cd-106	Cd-108	Cd-110	Cd-111	Cd-112	Cd-113	Cd-114	Cd-116
1.2 %	0.9 %	12.4 %	12.8 %	24.0 %	12.3 %	28.8 %	7.6 %

Table 1: Isotopic composition of the natural cadmium foils from GoodFellow metals.

in the literature (Hermanne et al., 2010) and with ours (see below). Using Qaim et al. data, a specific activity of 25 kCi/g is calculated. The theoretical specific activity is equal to 82 kCi/g, assuming that tin-117m is the only nucleus in the final product. The difference is due to the presence of the ground state tin-117g and other stable or long-lived tin isotopes produced during the irradiation.

1.3. Motivations

The ARRONAX cyclotron (Nantes, France) is an accelerator dedicated to the production of radionuclides. It delivers α particles at 67.4 MeV with an intensity up to 70 μ A (Haddad et al., 2008). In this frame, our study focuses on the measurement of the experimental tin-117m production cross section up to 67.4 MeV from Cd-nat target. Two data sets have been already published in the literature for the Cd-nat(α ,x) reaction, showing some discrepancies between them (Qaim and Döhler, 1984, Hermanne et al., 2010). The advantage of using Cd-nat as target is its availability in metallic form from the Goodfellow company (Goodfellow, 2015), with a good purity and homogeneity. Our measurements will allow to get an additional data set to define the behaviour of this reaction, and to determine the other radionuclides produced during the irradiation. From these data, it will be also possible to extract values from the Cd-116(α ,3n)Sn-117m reaction since only two of the tin stable isotopes that compose the natural cadmium target (see table 1) can produce Sn-117m: Cd-114 and Cd-116. Using these data, it will be possible to calculate the production rate and the specific activity of the final product as a function of the α incident energy from 25 MeV to 65 MeV. For the specific activity calculation, TALYS 1.6 code calculations will be used to infer stable tin isotopes production. This will allow to find the best compromise between production yield and specific activity for tin-117m.

2. Materials and methods

2.1. Experimental set-up

The production cross section data are obtained using the stacked-foils method (Duchemin et al., 2015, Blessing et al., 1995), which consists of the

irradiation of a set of thin foils, grouped as patterns. Each pattern contains a target to produce the isotopes of interest. Each target is followed by a monitor foil to have information on the beam intensity thanks to the use of a reference reaction recommended by the International Atomic Energy Agency (IAEA-NDS, 2015). In our experiment, the monitor foil acts also as a catcher to stop the recoil atoms produced in the target foil. A degrader foil is placed after each monitor foil to change the incident beam energy from one target foil to the next one.

Each foil in the stack has been weighed before irradiation using an accurate scale ($\pm 10^{-5}$ g) and scanned to precisely determine its area. The thickness is deduced from these values, assuming that it is homogeneous over the whole surface. In this work, 10 μm thick copper and aluminium monitor foils, 10 μm thick cadmium target foils and 100 to 500 μm thick aluminium degrader foils were irradiated. The foils, with an isotopic abundance and chemical purity of 99.9 %, 99 %, 99.7 % and 99 %, respectively, were purchased from Goodfellow[®].

The ARRONAX cyclotron (Haddad et al., 2008) delivers alpha particle beams with an energy uncertainty of ± 0.61 MeV, as specified by the cyclotron provider using simulations. The beam line is under vacuum and closed using a 75 μm thick kapton foil. The stacks were located about 6.8 cm downstream in air. The energy through each target and monitor foils has been determined in the middle of the thickness of the foil using the SRIM software (Ziegler et al., 2010). Energy loss in the kapton foil and air have been taken into account in our analysis.

All along the stack, depending on the number of foils, the energy uncertainty calculated using the SRIM software (Ziegler et al., 2010) increases up to ± 2 MeV due to the energy straggling (see table 2). Three stacks were irradiated to cover the energy range from 65 MeV down to 25 MeV (see table 2), which corresponds to the energy range of interest for the $\text{Cd-116}(\alpha,3n)$ reaction. Since the incident α beam energy delivered by the cyclotron is fixed, in two cases the first foil of the stack was a degrader foil in order to have a different energy through the first cadmium target foil. In addition, the use of several stacks allows also us to minimize the energy uncertainty in our experiment.

With natural cadmium and α particle as projectile, Sn-117m can be produced from nuclear reactions on Cd-116 or Cd-114. Cd-114 has its maximum contribution between 10 and 25 MeV. This region was not achievable in our experiments without large uncertainties on the projectile energy (higher than

2 MeV). We have then decided to restrict ourselves to 25 MeV, missing most of the contribution of Cd-114.

Irradiations were carried out with a mean beam intensity between 140 and 200 nA particles during one hour. Irradiation conditions are reported also in table 2.

For all the experiments, the recommended cross sections (Tárkányi et al., 2001) of the Cu-nat(α,x)Ga-67 (up to 50 MeV) or Al-27(α,x)Na-22 (from 50 MeV to 70 MeV) reactions were used to get information on the beam intensity.

There is a drawback in using a relative calculation, regarding the possible change in the recommended values when new more accurate measurements are available. The same problem exists for radioactive constants, γ emission branching ratios, etc. Being aware of this problem, we decided to mention the mean energy crossed by each monitor foil, for which our data have been obtained (see table 2). If the recommended values change (Tárkányi, F. et al., 2001) in the coming years, the cross section data can be modified accordingly.

Beam energy (MeV)	<Intensity> (nA p.)	Energy points in cadmium (MeV)		Energy points in monitor foils (MeV)	
67.40 (61)	196	65.01 (68)	55.13 (93)	64.58 (69)	54.65 (96)
67.40 (61)	199	48.92 (108)	35.43 (152)	47.41 (111)	33.06 (155)
67.40 (61)	143	45.86 (116)	39.51 (137)	45.06 (118)	38.61 (139)
67.40 (61)	158	42.10 (125)	29.25 (176)	41.26 (127)	28.10 (179)
			25.26 (193)		24.02 (199)

Table 2: Irradiation conditions and energies through the cadmium target foils and monitor foils estimated with SRIM (Ziegler et al., 2010)

During irradiation, an instrumented beam stop is used to control the beam current stability. However, it is not used as a faraday cup with precise intensity measurements, since it is not equipped with an electron suppression device.

The activity measurements in each foils were performed using a high purity germanium detector from Canberra (France) with low-background lead and copper shielding. All foils were counted twice. The first measurements started the day after the irradiation (after a minimum of 15 hours cooling time) during one hour, for all target and monitor/catcher foils. The second series of measurements were performed one week after EOB, during a minimum of 24 hours (one day) and up to 60 hours. Gamma spectra were recorded in a suitable geometry calibrated in energy and efficiency with standard Co-57,60 and Eu-152 gamma sources from LEA-CERCA (France). The full widths at half maxima were 1.04 keV at 122 keV (Co-57 γ ray) and 1.97 keV at 1332 keV (Co-60 γ ray). The samples were placed at a distance of 19 cm from the detector which is suitable to reduce the dead time and the effect of sum peaks. The dead time during the counting was always kept below 10%.

2.2. Data processing

All the activity values extracted for the radionuclides produced in the targets were derived from the γ spectra and the nuclear decay data (Kinsey et al., 1996, Ekström and Firestone, 2004), given in table 6 for both tin and cadmium isotopes, and in table 7 for indium isotopes. The spectra were analysed using the Fitzpeaks spectroscopy software (FitzPeaks Gamma Analysis and Calibration Software version 3.66).

The recoil nuclei coming from the cadmium targets have been detected and quantified in the monitor foils located after each target. In our experiment, the monitor foils are also used as catcher foils. The activity detected in each monitor foil has been added to that obtained in the preceding target foil.

By knowing the thickness of the foil precisely and the total activity of each isotope produced in the target, their production cross sections are calculated using the activation formula (1) with the appropriate beam current.

$$\sigma(E) = \frac{Act \cdot A}{\chi \cdot \phi \cdot N_a \cdot M \cdot (1 - e^{-\lambda t})} \quad (1)$$

In equation (1), the production cross section σ (mb) of a radionuclide at a given energy depends on its measured activity corrected to the time at the end of irradiation Act (Bq), its decay constant λ (s^{-1}), its atomic mass A ($g \cdot mol^{-1}$), its areal density M ($g \cdot cm^{-2}$), its chemical and isotopic abundance χ , the Avogadro constant (N_a), the irradiation duration t (s) and the beam current ϕ ($p \cdot s^{-1}$).

In our experiment, and because we use thin foils, each target foil receives the same beam current as the monitor foil placed behind it. It is then possible to define a relative equation (2) in which the knowledge of the beam current is no longer necessary. In this equation, the prime parameters are associated with Ga-67 or Na-22, used as isotopes of interest for the recommended cross section, while the others relate to the radionuclide produced in the target.

$$\sigma(E) = \sigma'(E') \cdot \frac{\chi' \cdot Act \cdot A \cdot M' \cdot (1 - e^{-\lambda t})}{\chi \cdot Act' \cdot A' \cdot M \cdot (1 - e^{-\lambda t})} \quad (2)$$

The cross section uncertainty is estimated with a propagation error calculation. Since all the parameters of equation (2) are independent, the total error is expressed as a quadratic sum (see equation (3)).

$$\frac{\Delta\sigma}{\sigma} = \sqrt{\left(\frac{\Delta\sigma'}{\sigma'}\right)^2 + \left(\frac{\Delta Act}{Act}\right)^2 + \left(\frac{\Delta Act'}{Act'}\right)^2 + \left(\frac{\Delta M}{M}\right)^2 + \left(\frac{\Delta M'}{M'}\right)^2} \quad (3)$$

The main error sources come from the recommended cross section values, the activity value of each produced radionuclide and the areal density uncertainties. The contribution of the irradiation time uncertainty is not significant and has been neglected. Since no uncertainty is given for the recommended cross section values, we have decided to use the uncertainty of the nearest experimental value used by the IAEA to perform the adjustment. It leads to an uncertainty of 11 % in average. The uncertainties on the activity of the radionuclides produced in the cadmium targets depend on different parameters such as the gamma line branching ratio, half-life, etc., described afterwards. These uncertainties are, in average, of 1.6 % for the tin-117m activity, 1.9 % for the Ga-67 activity and 10.5 % for the Na-22. Around 1 % of uncertainty is calculated for the areal density.

2.3. Thick Target production Yield (TTY)

Using the cross section values as a function of the energy $\sigma(E)$ obtained either in this work or in database, we have calculated the associated Thick

Target production Yields in MBq for one hour of irradiation and 1 μAe , also called 1h-1 μA yield. The values are obtained as a function of the projectile energy, using the following expression:

$$TTY = \phi \cdot \chi \cdot \frac{N_a \cdot \rho}{A} (1 - e^{-\lambda \cdot t}) \int_{E_{min}}^{E_{max}} \frac{\sigma(E)}{\frac{dE}{dx}} dE \quad (4)$$

In relation (4), ϕ represents the number of particles per second delivered in one μAe . The irradiation time, t , is set at one hour. χ corresponds to the isotopic abundance and chemical purity of the target, ρ is the target density ($\text{g}\cdot\text{cm}^{-3}$) and N_a is the Avogadro number. $\frac{dE}{dx}$ is the linear energy transfer of the projectile in the target material ($\text{MeV}\cdot\text{cm}^{-1}$). In a thick target, the incident particle energy decreases with the penetration depth. E_{max} corresponds to the incoming projectile energy, whereas E_{min} corresponds to its energy after the target.

2.4. Comparison with the TALYS 1.6 code

In this work, all the experimental cross section values are compared with the latest version (1.6) of the TALYS code released in December, 2013 (Konig and Rochman, 2012). TALYS is a nuclear reaction program which simulates reactions induced by light particles on nuclei heavier than carbon. It incorporates theoretical models to predict observables including cross section values as a function of the incident particle energy (from 1 keV to 1 GeV). A combination of models that best describes the whole set of available data for all projectiles, targets and incident energies have been defined by the authors and put as default in the code. In this way, a calculation can be performed with minimum information in the input file: the type of projectile and its incident energy, the target type and its mass. The results are plotted as TALYS 1.6 default in the following figures. Since there are some differences between experimental data and the results of the TALYS code using default models, we have defined a combination of models, already included in the TALYS code, that better describes the production cross sections, for a variety of projectiles, incident energies and target masses.

The description of the optical, preequilibrium and level density models have been found to have a great influence on the calculated production cross section values. Better results are, in general, obtained when alpha particles are used as projectile using the optical model described by Demetriou et al. (Demetriou et al., 2002), a preequilibrium model based on the exciton

model including numerical transition rates with optical model for collision probabilities (Gadioli and Hodgson, 1992) and a model for the microscopic level density from Hilaire’s combinatorial tables (Goriely, Hilaire and Konig, 2008). The results of this combination of models are referenced in the following figures as TALYS 1.6 Adj.

3. Results and discussions

This part shows the experimental production cross section results for the Cd-nat(α ,x) reactions. The determination of the Cd-116(α ,3n)Sn-117m production cross section values and Sn-117m specific activity is then detailed.

3.1. The Cd-nat(α ,x)Sn-117m production cross section

Tin-117m ($T_{1/2} = 13.60$ (4) d) decays by Isomeric Transition (IT) to its stable ground state tin-117g by emitting γ rays at 156 and 158 keV (see table 6). The activity extracted from both γ lines were in good agreement. Our tin-117m production cross section results are plotted in figure 1 as full points.

As reported in table 6, tin-117m is produced in the natural cadmium material from the Cd-114(α ,n) reaction with an energy threshold of 5.4 MeV and from the Cd-116(α ,3n) reaction with an energy threshold of 20.8 MeV. Our results show a maximum around 80 mb and 35 MeV, mainly coming from the Cd-116(α ,3n) reaction. The peak at low energy, which is related to Cd-114, is not visible in our data set due to our minimal alpha particle energy of 25 MeV.

Two other data sets have been published in the literature (Qaim and Döhler, 1984, Hermanne et al., 2010). The one published in 1984 gives values in the energy range from 15 MeV to 137 MeV and the other one, published in 2010, in the energy range from 5 MeV to 38.5 MeV. These series are shown in figure 1 as rhombs and boxes, respectively, up to 80 MeV. Qaim and Döhler, 1984, made a high energy range study and figure 1 shows only the lower energy part. The points of Qaim and Döhler have been degraded rather far from the initial energy, which explains the energy shift of around 10 MeV in comparison to Hermanne et al.

Our data are in good agreement with those published by Hermanne et al., 2010, and with the energy thresholds of the reactions contributing to the tin-117m production. Our new set of data complements the trend obtained with the experimental data points from Hermanne et al., 2010. The knowledge of the Cd-nat(α ,x)Sn-117m excitation function is then better described between

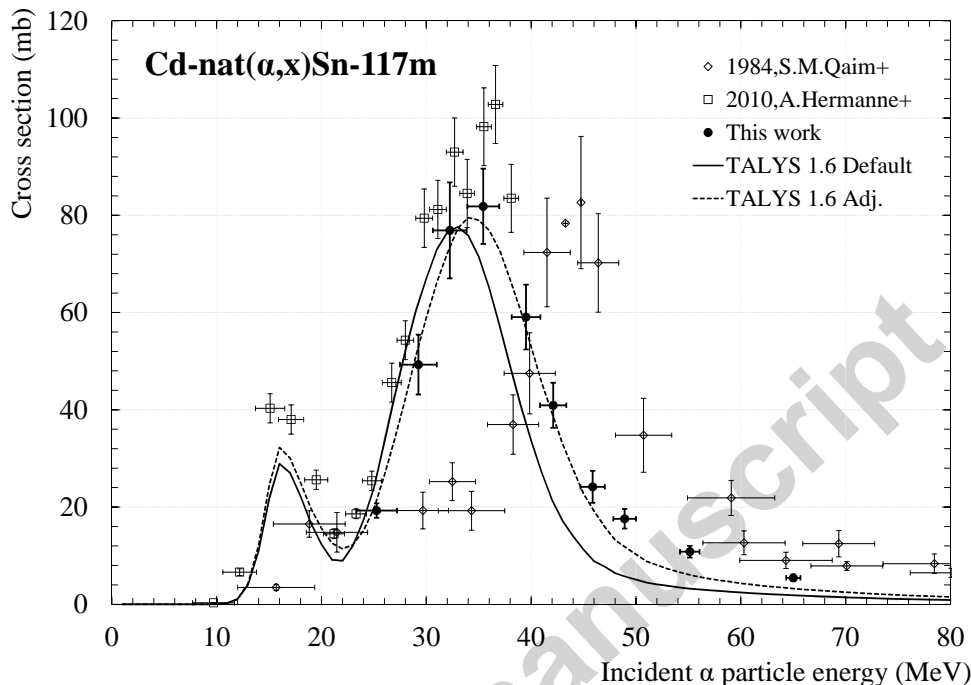


Figure 1: Cd-nat(α,x)Sn-117m excitation function

38 and 65 MeV. With our data and those published in 2010, the contribution from both Cd-114 and Cd-116 to the tin-117m production with a natural cadmium target are well described.

The experimental data are compared with the results of the TALYS code version 1.6 with default (full line) and adjusted (dash line) models. As an overall result, the TALYS code confirms the trend exhibited by the experimental data. The results from TALYS 1.6 Adj. well follow the experimental trend in energy and amplitude, whereas TALYS 1.6 Default shows an energy shift of a few MeV toward low energies.

3.2. The tin-117m contaminants production cross sections

3.2.1. The Sn-110 production cross section

Tin-110 has a half-life of 4.154 (4) hours (IAEA-NDS, 2015). It decays by electronic capture to the metastable state of indium-110 ($T_{1/2} = 69.1$ (5) minutes), by emitting an intense gamma ray of 280.459 keV (97.06 (8) %). This gamma line was used to determine its activity in the recorded gamma spectrum. Tin-110 is produced by (α,xn) reactions on different isotopes in

the natural cadmium target, from Cd-108 to Cd-113 in our energy range of interest (see table 6). Our data are presented in figure 2 and table 8.

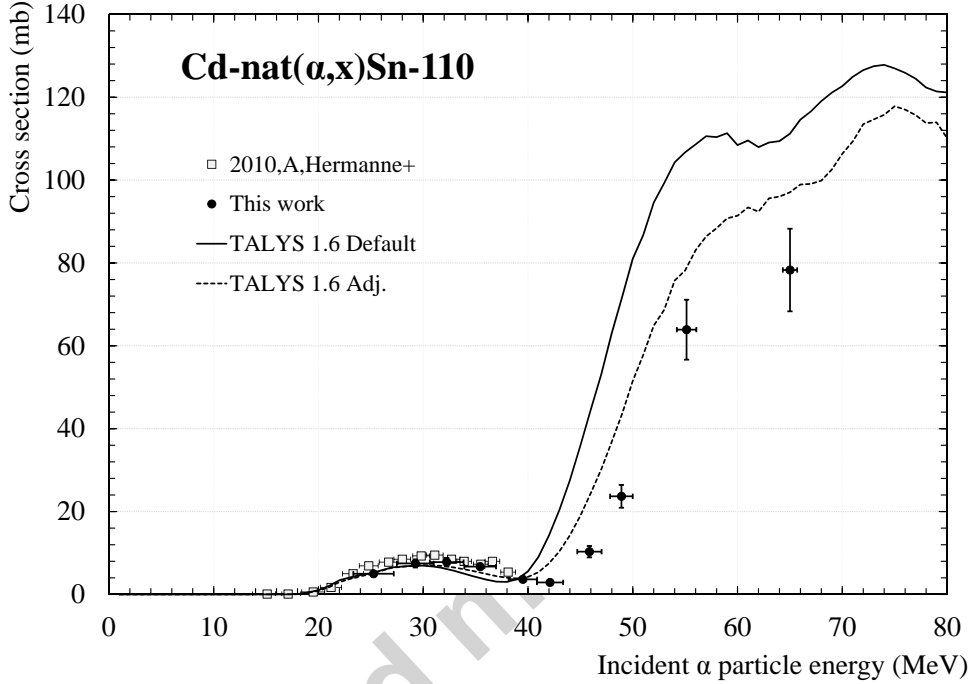


Figure 2: Cd-nat(α ,xn)Sn-110 excitation function.

Our results are the first ones, for this isotope, above 38 MeV. Below this energy, the agreement with Hermanne et al., 2010, is good. TALYS is able to reproduce the trend. Moreover, the amplitude is well reproduced with TALYS 1.6 Adj.

3.2.2. The Sn-113 production cross section

Tin-113 can be produced either in the ground state, Sn-113g, or in the isomeric state, Sn-113m. Sn-113m has a short half-life of 21.4 (4) minutes. It decays by electronic capture (8.9 %) to In-113g (stable) and by isomeric transition (91.1 %) to Sn-113g. Sn-113g, on the other hand, has a long half-life of 115.09 (4) days and decays by electronic capture and β^+ emission to In-113, which emits a high intensity gamma line at 391.690 keV. This gamma ray has been used to determine its activity (see table 6). Tin-113m has not been detected in our targets. Its half-life is so short that the 15 hours cooling

time between the end of bombardment and our measurements has not allowed to quantify its remaining activity during our first measurements. The Sn-113g activity measured is then cumulative, including that of Sn-113m. After one to two weeks cooling time, and 24 to 64 hours of counting time, the Sn-113g cumulative activity has been extracted with an uncertainty of 3.9 % in average. Our values are presented in figure 3 and table 8.

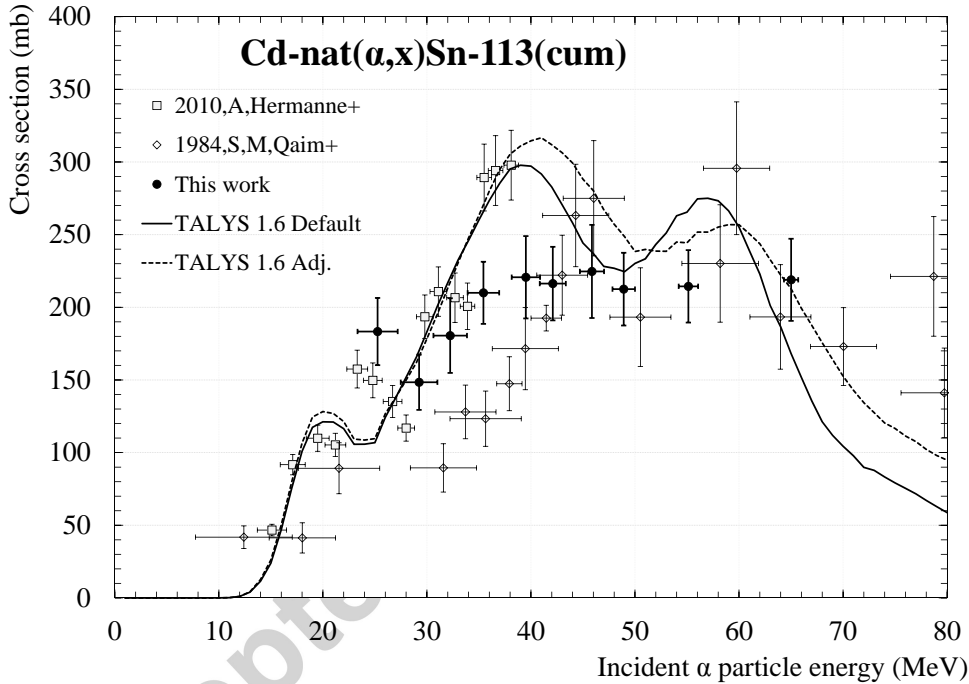


Figure 3: Cd-nat(α ,xn)Sn-113 excitation function (cumulative).

Our data allow to highlight the end of the Cd-111(α ,2n) contribution ($E_s = 15.17$ MeV), that of Cd-112(α ,3n) from 24.90 MeV and Cd-113(α ,4n) from 31.66 MeV (see table 6). However, other measurements are needed to better discriminate the other reaction contributions at higher energies. The data in literature (Qaim and Döhler, 1984, Hermanne et al., 2010) are not in agreement. This difference has been already discussed for the tin-117m production cross section. We observe some differences in the amplitude between our data and those published by Hermanne et al. in 2010. However, looking at the article (Hermanne et al., 2010), our results are comparable since in both cases the Sn-113g production cross section is cumulative and

the 391 keV gamma line is used to extract the Sn-113g(cum.) activity. The experimental results are too dispersed to conclude on the results of both combinations used in the TALYS code.

3.2.3. The In-109 production cross section

In-109 is produced by Cd-nat(α ,xn+p) reactions. In-109g ($T_{1/2} = 4.2$ (1) h) is also arising from the decay of its metastable states, In-109m2 ($T_{1/2} = 0.209$ (6) s) and In-109m1 ($T_{1/2} = 1.3$ minutes), and the decay of Sn-109 ($T_{1/2} = 18$ min). The 15 hours cooling time between the end of irradiation and the first measurements allowed the decay of the In-109m2, In-109m1 and Sn-109 nuclei produced during the irradiation. The In-109g activity values obtained from our spectra are then cumulative. In-109g has been identified and quantified using the 203.5 keV (74 %) γ ray emitted from its decay. It emits other γ lines with low branching ratio that led to high uncertainties. These lines were not used in the activity calculation but they allowed to validate the values given by the 203.5 keV γ line. Our data are listed in table 8 and depicted in figure 4.

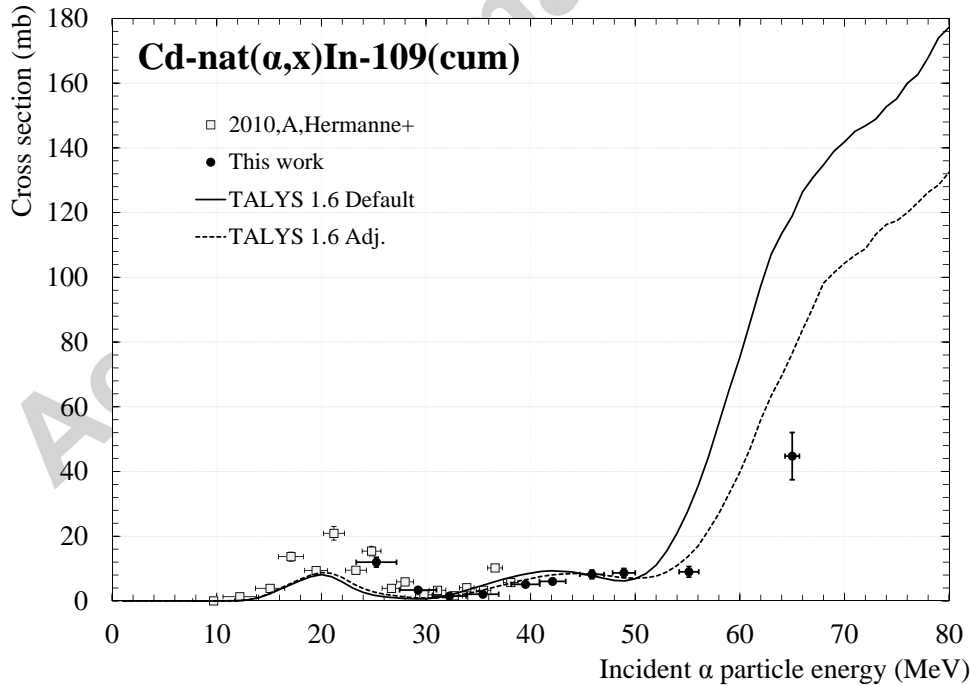


Figure 4: Cd-nat(α ,x)In-109 excitation function (cumulative).

Our experimental data follow the trend made by the points published in 2010 by Hermanne et al. and give additional information from 38 MeV to 65 MeV. The different reaction contributions (see table 7) are well defined both by our experimental points and the TALYS code. The TALYS Adj. results are closer to our experimental points than TALYS 1.6 Default, above 55 MeV. Under 30 MeV, TALYS gives underestimated results. Between both energies, the code gives satisfactory results.

3.2.4. *The In-110 production cross section*

In-110 has a metastable state, In-110m, with a half-life of 69.1 (5) minutes. This half-life is too short to obtain information on the produced activity, considering our experimental conditions. In-110m decays by EC/ β^+ emission to Cd-110 (stable). The activity of the In-110 ground state (In-110g) has been obtained using the γ lines summarized in table 7. In-110g is not subject to the decay of Sn-110, which decays at 100 % to In-110m. Our numerical cross section values are presented in figure 5 and table 9. Our values are in agreement with those published in 2010 by Hermanne et al. Above 50 MeV, additional measurements are needed to better describe the experimental trend. Up to 50 MeV, TALYS 1.6 Adj. gives good results.

3.2.5. *The In-111 production cross section*

The decay of the indium-111 ground state ($T_{1/2} = 2.8047$ (5) days) leads to the emission of two gamma rays (see table 7) with high branching ratios, which are easily detectable. Cross section results are presented in figure 6 and table 9. They are cumulative values that include contributions from Sn-111 ($T_{1/2} = 35.3$ (6) min) and In-111m ($T_{1/2} = 7.7$ (2) min). These results allow to expand our knowledge on the In-111 production with the irradiation of a natural cadmium target by α particles, especially between 40 and 70 MeV. Our results are in agreement with the energy threshold of the different nuclear reactions identified as possible source (see table 7). There is a small shift in the energy between our data and those of Hermanne et al between 30 MeV and 50 MeV. The TALYS code is able to reproduce the experimental trend.

3.2.6. *The In-114m production cross section*

In-114 has two metastable states, In-114m2 ($T_{1/2} = 43.1$ (6) s) and In-114m1 ($T_{1/2} = 49.51$ (1) d), and an unstable ground state In-114g ($T_{1/2} = 71.9$ (1) s). In-114m2 decays at 100 % to In-114m1 by internal transition.

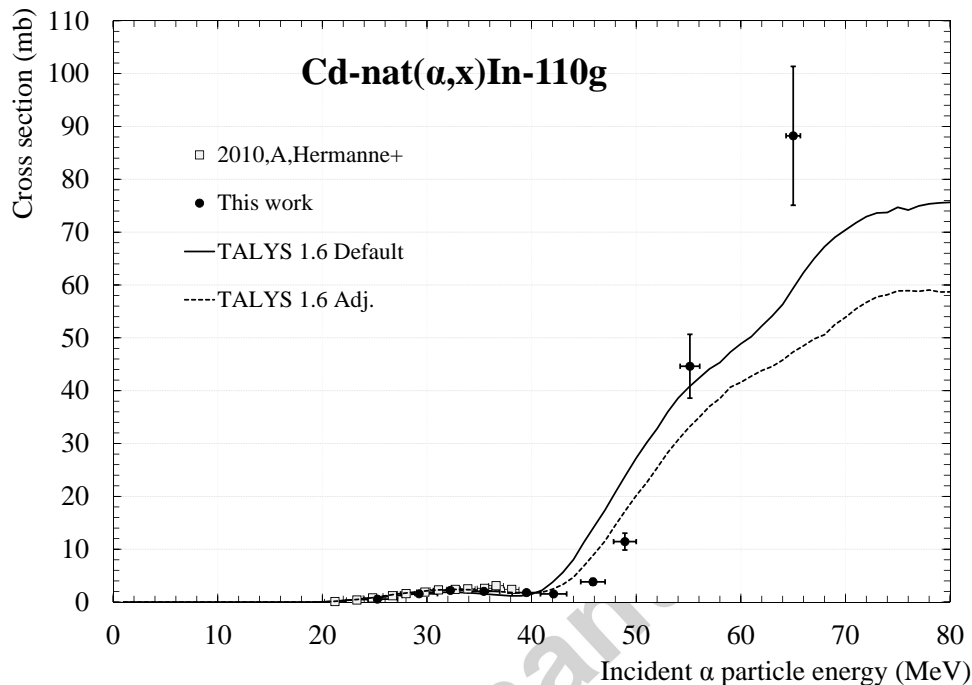


Figure 5: Cd-nat(α,x)In-110g excitation function

The In-114m1 activity has been obtained from the gamma lines summarized in table 7. In-114g half-life is $5.6 \cdot 10^4$ times lower than that of In-114m1. Both activities are quickly in secular equilibrium. The cross section values deduced from these activity values are cumulative and are presented in table 9 and figure 7. Our cross section results show a good agreement with those of Hermanne et al. up to 35 MeV. Above this energy, our data are the first to give additional information on the trend. TALYS gives the good trend. Above 55 MeV, TALYS 1.6 Adj. well estimates the excitation function amplitude.

3.2.7. The Cd-115g production cross section

Cd-115 has a ground state, Cd-115g ($T_{1/2} = 53.46$ (10) hours), which is not subject to the decay of its metastable state, Cd-115m ($T_{1/2} = 44.6$ (3) days). Cd-115g decays to In-115 by emitting different gamma rays common with Cd-115m, even though Cd-115m has not been quantified due to the low branching ratio of its gamma lines. The γ line at 527.9 keV (see table 6) was used to determine the Cd-115g activity since it is the only detectable gamma

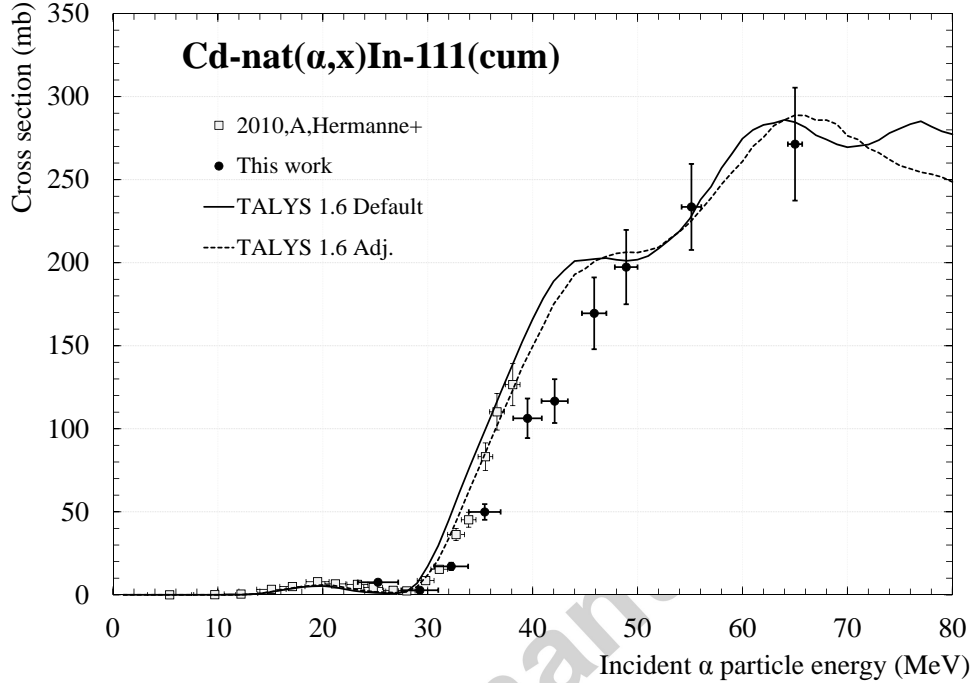


Figure 6: Cd-nat(α,x)In-111 excitation function

line different from the Cd-115m ones. Cross section data are presented in table 9 and figure 8.

Our experimental data well reproduce the ($\alpha, 2p+xn$) reactions contribution, with a shoulder around 40 MeV. Our work is the first one to study the Cd-116($\alpha,2p+3n$) reaction from threshold (38.27 MeV) up to 65 MeV. Indeed, the values published in 2010 by Hermanne et al. are up to 38 MeV and depends only on the Cd-116($\alpha,\alpha+n$) and Cd-114($\alpha,2p+n$) reactions. Both sets of data are in good agreement between them. Experimental data are compared with the TALYS code, which is not able to reproduce the experimental trend for these ($\alpha,2p+xn$) reactions.

3.2.8. The experimental Cd-nat(α,x) reactions production Yields

The production yield values are presented in figure 9 for all detected and quantified isotopes in the natural cadmium target. These data have been obtained from equation 4 and from our experimental cross section results.

Sn-110, Sn-113g, In-109, In-110, In-111 are the isotopes which mainly lead to the decrease of the Sn-117m radionuclidic purity in natural cadmium. At

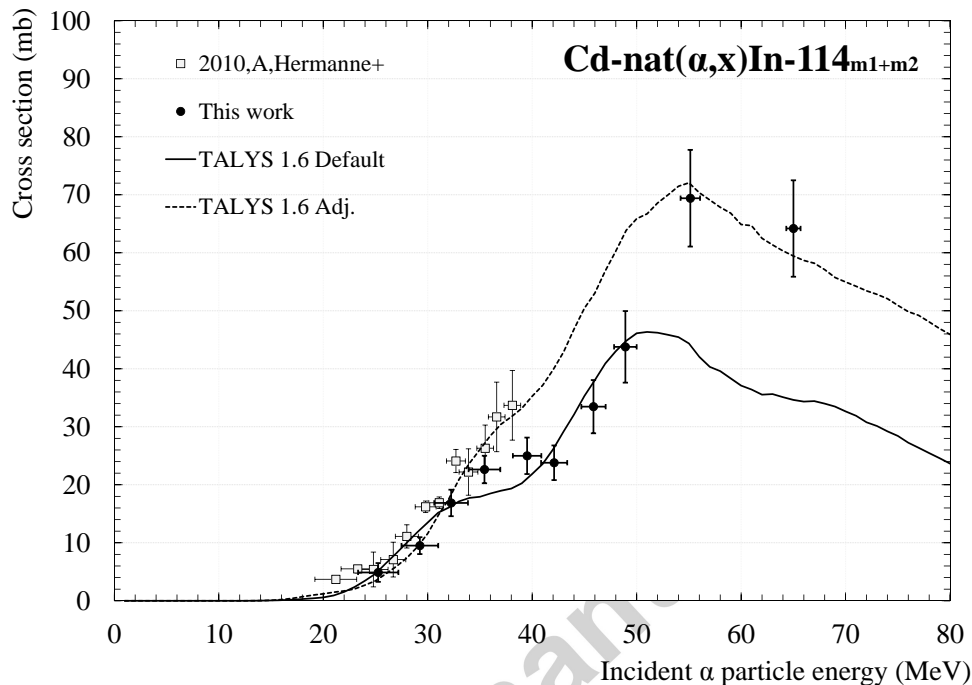


Figure 7: Cd-nat(α,x)In-114m1+m2 excitation function

60 MeV, the In-111 and Sn-110 production yields are, respectively, 17 and 44 times higher than that of Sn-117m. Indium isotopes can be eliminated by chemical separation. Sn-110 and Sn-113g can be avoided using enriched cadmium as target material and appropriate incident beam energy.

3.3. The tin-117m production from the Cd-116($\alpha,3n$) reaction

As described in the material and method part, in natural cadmium only Cd-114 and Cd-116 can contribute to the production of tin-117. Cd-114 has its main contribution at low energy as it can be seen from data published by Adam Rebeles et al. in 2008 (Adam Rebeles et al., 2008) on the energy range from 12 to 38 MeV. The contribution of Cd-114 can be estimated and subtracted from the values obtained from Cd-natural, to get a new evaluation of the Cd-116($\alpha,3n$) contribution. The data obtained for the Cd-116($\alpha,3n$) reaction have then been compared with the existing ones, both for cross section and thick target production yield values. Using the TALYS code, all the other tin isotopes produced during the irradiation have been considered

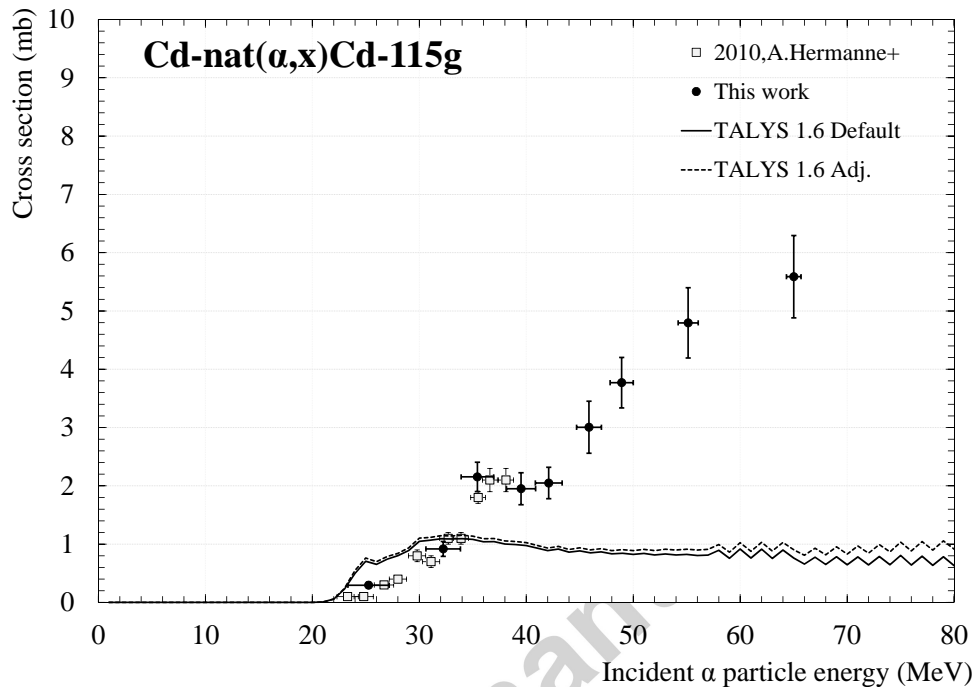


Figure 8: Cd-nat(α,x)Cd-115g excitation function

including stable tin isotopes, which allows to calculate the specific activity as a function of the projectile energy.

3.3.1. Determination of the Cd-116($\alpha,3n$)Sn-117m excitation function

Data exist in the literature for the Cd-114(α,n) excitation function. They have been published by Adam Rebeles et al. in 2008 (Adam Rebeles et al., 2008) on the energy range from 12 to 38 MeV. Up to the energy threshold of the Cd-116($\alpha,3n$) reaction, i.e. 20.8 MeV, it is the only contribution for the production of Sn-117m. The first step was, therefore, to scale down the data from Adam Rebeles et al., 2008, by multiplying the values by the isotopic abundance of Cd-114 in natural Cd (28.8 % - see table 1). These scaled data are presented in figure 10. Data from Hermanne et al., 2010, are also used, up to the Cd-116($\alpha,3n$) energy threshold.

In figure 10, values from the TALYS code 1.6 Adj. are presented as dashed line. These values correspond to a natural abundance in Cd-nat of 28.8%. TALYS values are lower than the experimental ones even if they show a similar behaviour. In order to get information on the Cd-114(α,n)

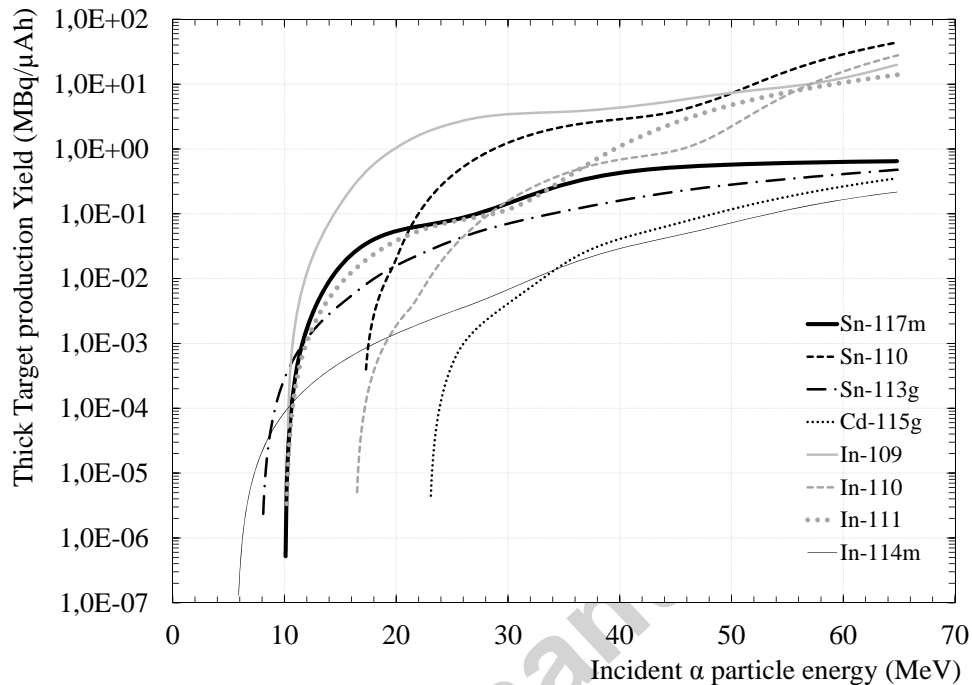


Figure 9: Production Yield calculated for $1 \mu\text{Ae}$ and 1 hour of irradiation, from our experimental cross section values obtained for $\text{Cd-nat}(\alpha, x)$ reactions.

production cross section at higher energy, we have decided to use the TALYS 1.6 adj. results, applying a coefficient to bring these values close to the experimental data.

In figure 10, the full line shows the behaviour of the normalized values of the TALYS code. The agreement between the data and the normalized value is very good. These data can then be used to calculate the $\text{Cd-114}(\alpha, 3n)\text{Sn-117m}$ cross section values up to 65 MeV. These values, called "TALYS 1.6 Adj. - with the amplitude adjusted to the experimental values" in figure 10, are used to determine the contribution of the $\text{Cd-114}(\alpha, n)$ reaction from our experimental data obtained using natural cadmium. 13 % of uncertainty is considered on the normalized and adapted values from TALYS, corresponding to the larger uncertainty on the experimental data of Adam Rebeles et al. (Adam Rebeles et al., 2008) and Hermanne et al. (Hermanne et al., 2010) used to fix the TALYS trend. After subtraction of this contribution from our $\text{Cd-nat}(\alpha, xn)\text{Sn-117m}$ cross section results, the obtained data are normalized to take into account the fact that Cd-116 represents only 7.6 % of the atoms

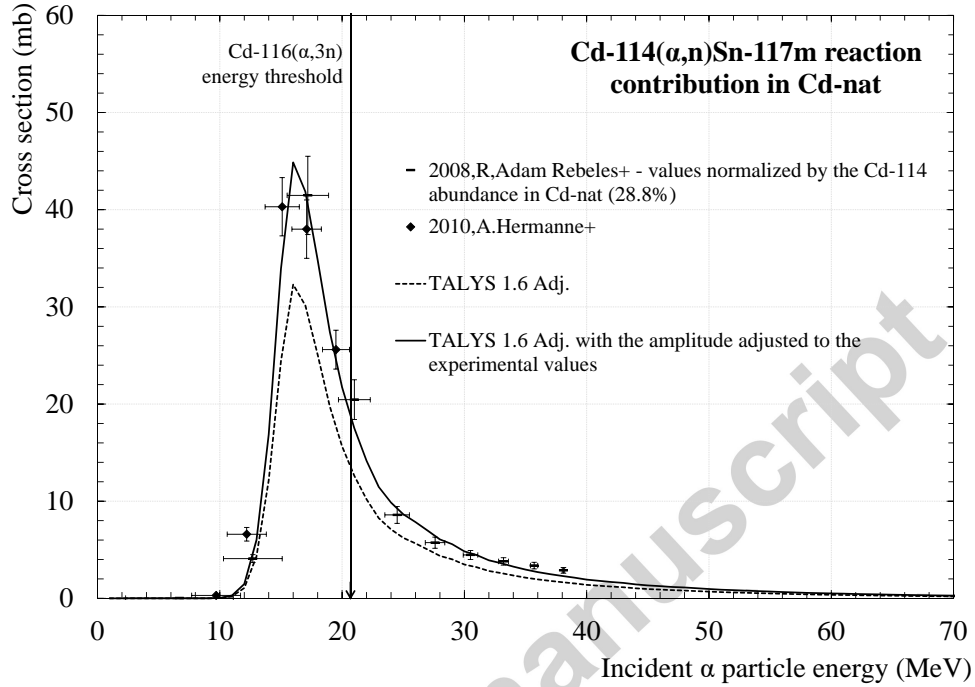


Figure 10: Cd-114(α,n)Sn-117 excitation function normalized to a Cd-nat target

in the natural cadmium target. Our calculated data are plotted as crosses in figure 11 and the numerical values are listed in table 3.

Energy (MeV)	σ Sn-117m (mb)
65.01 ± 0.68	66.61 ± 9.18
55.13 ± 0.93	133.23 ± 15.95
48.92 ± 1.08	218.20 ± 26.59
45.86 ± 1.16	301.13 ± 43.41
42.10 ± 1.25	516.54 ± 61.05
39.51 ± 1.37	750.52 ± 87.69
35.43 ± 1.52	1038.63 ± 101.98
32.24 ± 1.61	961.22 ± 130.13
29.25 ± 1.76	577.68 ± 81.51
25.26 ± 1.93	142.56 ± 35.05

Table 3: Tin-117m production cross section values from the Cd-116($\alpha,3n$), deduced from our experimental data obtained for the Cd-nat(α,x)Sn-117m reaction.

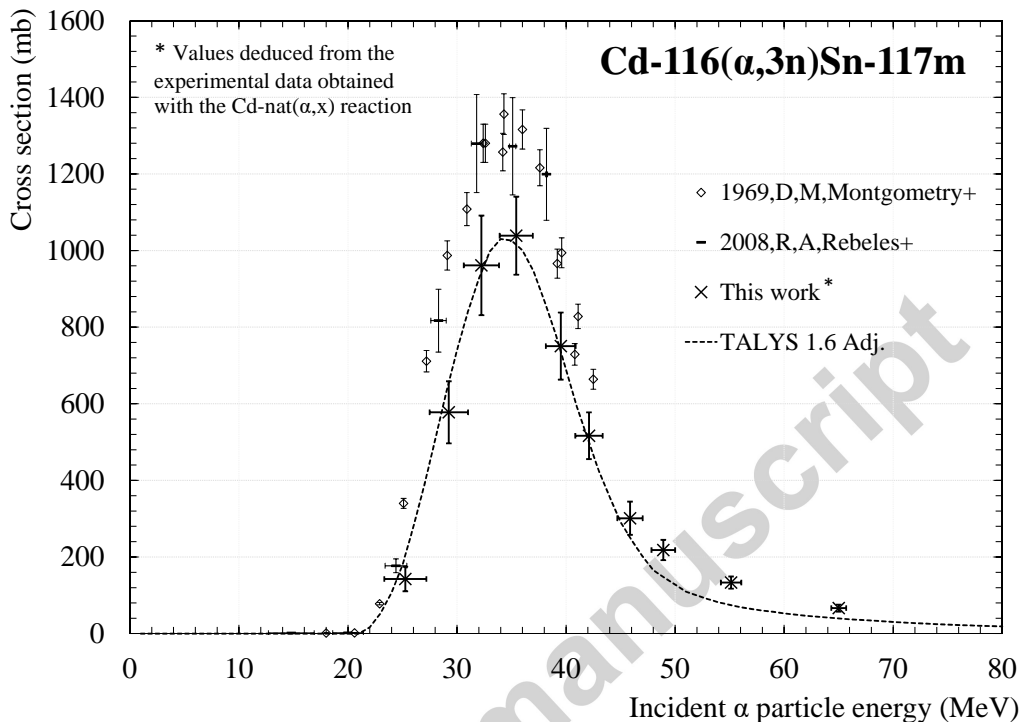


Figure 11: Cd-116($\alpha,3n$)Sn-117m excitation function.

Our values for the Cd-116($\alpha,3n$)Sn-117m cross section show a maximum at 36 MeV of around 1 barn. The two published set of data (Montgomery and Porile, 1969, Adam Rebeles et al., 2008) show similar results with a maximum around 36 MeV. However, in comparison with our data, their maximum value is 13 % higher than ours. The authors of the experiments published in 1969 and 2008 have determined the Cd-116($\alpha,3n$)Sn-117m production cross section using electroplating method for the target preparation, and enriched Cd-116 material (respectively 97.2 and 97.7 %).

For the Cd-nat(α,x) reaction, the cross section values from our work and those of Hermanne et al., 2010, show the same amplitude. Data from Adam Rebeles et al., 2008, normalized for a Cd-nat target are 20 % higher. Furthermore, in the article published by Montgomery and Porile, 1969, the γ lines used to extract the Sn-117m activity are presented at 159 and 161 keV. Today, the energy values tabulated in the nuclear data bases (Kinsey et al., 1996, Ekström and Firestone, 2004) are different. Their data will also

strongly depend on the target homogeneity and the Cd-116 isotopic purity.

In our case, our calculation strongly depends on the experimental data obtained with the Cd-nat target and on the adjusted TALYS values for the Cd-114(α ,n) reaction (see figure 10). The values obtained in the energy range between 25 and 30 MeV are the most dependent to the Cd-114(α ,n) reaction, as shown in figure 10.

Our Cd-116(α ,3n)Sn-117m excitation function results shown in figure 11 are in good agreement with the TALYS 1.6 Adj. results. They give the same energy and value for the maximum of the cross section.

3.3.2. The tin-117m Thick Cd-116 Target production Yield

The Thick Target production Yield (*TTY*) is calculated using the relation shown in part 2.3 after applying a spline interpolation on the experimental data points. First, a fit from the Montgomery and Porile, 1969 and Adam Rebeles et al., 2008, cross section values has been done. From this fit, the thick target production yield has been calculated and is presented in figure 12 as a function of the incident α particles energy. It reaches 6.1 MBq/ μ Ah at 42.5 MeV, the maximal energy available with experimental data. Secondly, a fit is applied to our data assuming a 100 % Cd-116 enriched target. The thick target production yield reaches 4.4 MBq/ μ Ah at 42.5 MeV (see figure 12), which corresponds to 72 % of the value obtained with the literature data (Montgomery and Porile, 1969, Adam Rebeles et al., 2008).

The Clear Vascular company produces tin-117m using the Cd-116(α ,3n) reaction with 99 % Cd-116 enriched target. The corresponding Thick Target production Yield over the energy range 47 MeV down to 20 MeV is consistent with 150 μ Ci/ μ Ah, or 5.55 MBq/ μ Ah (Stevenson et al., 2015), determined using the data published in Qaim and Döhler, 1984. In one hand, for the same energy range, our work gives a value of 5.2 MBq/ μ Ah considering a 100 % Cd-116 enriched target. This value is close to that presented by the Clear Vascular Company (Stevenson et al., 2015). In the other hand, the yield obtained from the data published in 1969 and 2008 (Montgomery and Porile, 1969, Adam Rebeles et al., 2008) overestimates the value of Stevenson et al., 2015, for a reduced energy range from 42.5 MeV down to 20 MeV. Using a 65 MeV α particle beam with a Cd-116 target thick enough to decrease the incident energy down to 20.80 MeV (the Cd-116(α ,3n) energy threshold), the production yield reaches 6.3 MBq/ μ Ah from our data (see figure 12).

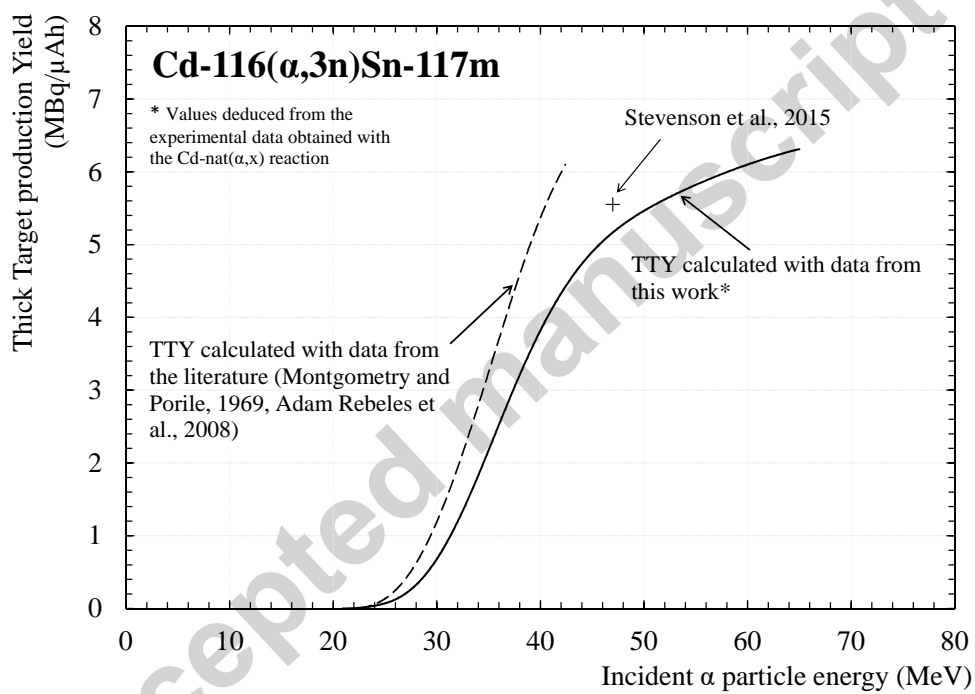


Figure 12: Cd-116($\alpha,3n$)Sn-117m production Yield calculated for 1 μ Ae and 1 hour of irradiation.

3.4. The tin-117m radionuclidic purity

Considering the production of other radioactive tin isotopes during the irradiation of a 100 % Cd-116 target, Sn-110 and Sn-111 will not be produced, since the energy threshold is higher than the energy considered in our study (65 MeV). However, tin-113 can be produced with the Cd-116(α ,7n) reaction from its energy threshold at 56.3 MeV. Tin-113 can be totally avoided with α particle energy beam under 56 MeV. With 56 MeV, the Sn-117m production yield reaches 92 % of that with 65 MeV, which corresponds to 5.8 MBq/ μ Ah. The best radioisotopic purity will be obtained, in this case, with 56 MeV α beam.

3.5. The tin-117m Specific Activity (SA)

3.5.1. The Specific Activity (SA)

The Specific Activity (SA) is the ratio between the activity of the radionuclide of interest and the total mass of all isotopes of the same element standing in the sample. The specific activity is usually expressed in term of activity per element quantity: Ci/mol, Ci/g, Bq/mol, Bq/g or MBq/nmol (see equation 5).

$$SA = \frac{Act_{isotope\ of\ interest}}{m_{isotopes\ of\ the\ same\ element}} \quad (5)$$

If all atoms standing in the sample are those of the radionuclide of interest, the SA is maximum. However, the irradiation of a target usually leads to the production of other stable or radioactive isotopes of the same element. In these cases, the SA value decreases. The SA is of relevance for radiolabeling and for radiopharmaceuticals, for the determination of their chemical and/or biological effect on the targeted system (IAEA, 2008). Indeed, if there are other isotopes than the one of medical interest, some vector molecules are labelled with these other isotopes, which will be inefficient.

With cyclotrons it is possible to reach high specific activities since the use of charged particles allows to produce a radionuclide of interest for which its chemical element is different to the one composing the target.

3.5.2. The Sn-117m SA determination method and discussion

For the tin-117m SA determination, the Sn-117m production yield is needed. This value has been determined previously from our experimental data. In addition, the mass of all tin isotopes is needed. First, we suppose that a chemical separation is made quickly after the EOB and that all the

remained isotopes in the product are Sn isotopes. Using a 65 MeV beam, Sn-113 to Sn-120 are produced. No data are available for stable isotopes. The production cross section values of all tin isotopes that can be produced with a 65 MeV α beam on a Cd-116 target have been determined using TALYS 1.6 Adj.

The SA is calculated at the EOB up to 65 MeV using the number of Sn-114,115,116,117g,118,119g,120 stable atoms and that of Sn-113m ($T_{1/2} = 21.4$ (4) min), Sn-113g ($T_{1/2} = 115.09$ (4) days) and Sn-119m ($T_{1/2} = 293.1$ (7) days). The values are plotted in figure 13 in kCi/g, as a function of the incident α particles energy. At EOB, the tin-117m SA reached 41.4 kCi/g at 39.4 MeV.

The mass contribution (%) of each Sn isotope is shown in table 4, for different energies impinging a Cd-116 target thick enough to decrease the initial energy down to the Cd-116($\alpha,3n$) energy threshold.

Energy	30 MeV	40 MeV	50 MeV	60 MeV
Sn-113m	0	0	0	0.0012
Sn-113g	0	0	0	0.00021
Sn-114	0	0	0.0050	1.71
Sn-115	0	0.0036	4.85	20.91
Sn-116	0.017	11.71	34.67	33.70
Sn-117g	6.43	5.42	3.47	2.54
Sn-117m	25.95	50.38	38.40	28.36
Sn-118	66.31	31.75	18.12	12.44
Sn-119m	0.58	0.33	0.22	0.16
Sn-119g	0.72	0.41	0.26	0.19
Sn-120	0.000092	0.000034	0.000018	0.000012

Table 4: Mass contribution in % of the Sn isotopes in the sample at EOB, for a Cd-116 target irradiated by different beam energies down to the Cd-116($\alpha,3n$) reaction threshold.

3.5.3. The Sn-117m SA from a commercialized Cd-116 enriched product

Trace Sciences International Inc. provides enriched material including Cd-116, with an isotopic composition presented in table 5.

Such information allows to calculate the specific activity based on a commercialized Cd-116 material, still starting from the Cd-116($\alpha,3n$) energy threshold.

Cd-106	Cd-108	Cd-110	Cd-111	Cd-112	Cd-113	Cd-114	Cd-116
0.01 %	0.01 %	0.25 %	0.25 %	0.71 %	0.38 %	1.79 %	96.6 %

Table 5: Isotopic composition of the Cd-116 enriched product provided by Trace Sciences.

Based on the fact that the amount of atoms of Cd-106, 108, 110 and Cd-111 is negligible (less than 0.3 %), only nuclear reactions on Cd-112,113,114 and Cd-116 are considered. Cd-114 and Cd-116 are the only Cd isotopes leading to the production of Sn-117m. The Sn-117m production yield obtained from our experimental data for a 100 % Cd-116 enriched target (see figure 12) is then normalized by the real percentage of Cd-116; 96.6 % (see table 5). For the Cd-114(α ,n) reaction the Sn-117m production is calculated from the production cross section of TALYS 1.6 Adj. normalized as presented in figure 10, and reduced by the percentage of Cd-114 in the enriched product. Both values are added.

The other Cd isotopes composing the enriched material lead to the decrease of the specific activity and radionuclidic purity by producing other Sn isotopes atoms. Based on the same method, previously presented, the number of atoms produced from the different Cd isotopes composing the enriched material has been calculated using the TALYS 1.6 Adj. code, normalized by their respective percentage.

This calculation gives a maximum Sn-117m specific activity at 39.5 MeV and 40.3 kCi/g, close to that obtained assuming a 100 % Cd-116 target (i.e. 39.4 MeV and 41.4 kCi/g). With the same target, the Sn-117m production yield reaches 6.1 MBq/ μ Ah at 65 MeV, against 6.3 MBq/ μ Ah with a 100 % Cd-116 target.

However, this isotopic composition reduces the radionuclidic purity by the production of the long half-life Sn-113g, that can be produced from 24.50 MeV with the Cd-112(α ,3n) reaction. Sn-113g is also produced below this energy if we consider the reactions on Cd-106 to Cd-111 atoms. Sn-113 has a metastable state, Sn-113m, that decays by isomeric transition to Sn-113g. Few hours after the EOB, Sn-113m has totally decayed and 91.1 % of the Sn-113m atoms have been transformed to Sn-113g atoms (see part 3.2.2). At that time and considering only the reactions on Cd-112,113,114 and Cd-116, the Sn-113g activity represents 0.16 % of the Sn-117m activity, against 0.008 % at the EOB (without Sn-113m decay).

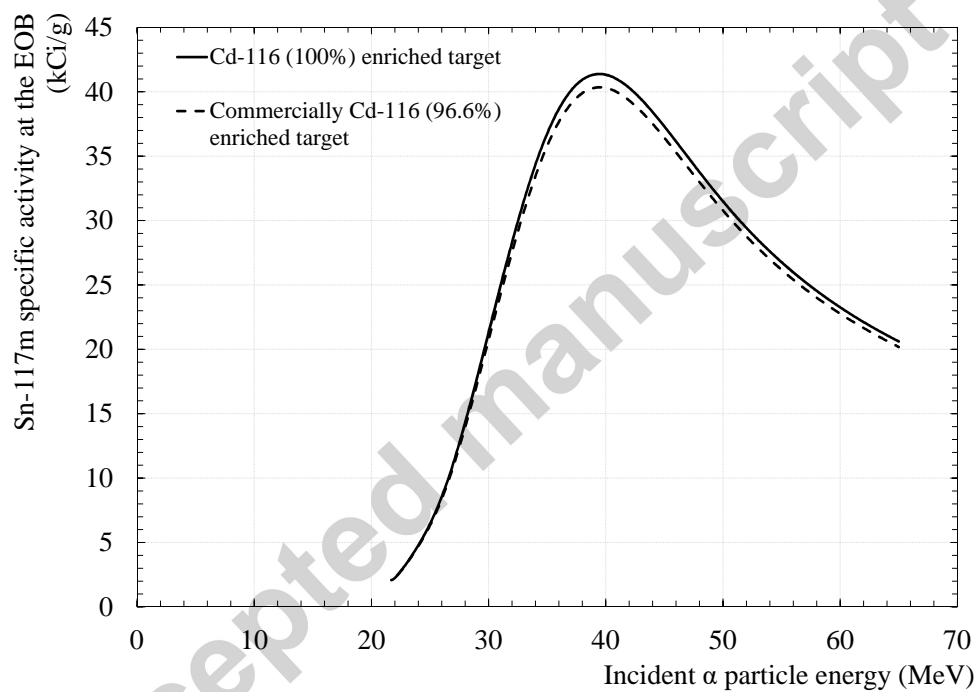


Figure 13: Tin-117m specific activity at the EOB calculated from a 100 % Cd-116 target (full line) and a commercialized Cd-116 enriched target (dash line), as a function of the incident α particles energy.

4. Conclusion

Tin-117m is a radionuclide of medical interest, already used in pre-clinical and clinical trials for vulnerable plaque. Previous studies have shown that the $\text{Cd-116}(\alpha,3n)$ reaction leads to the highest purity product, with a production rate in agreement with that required for medical applications. Due to the lack of data at an energy higher than 42.5 MeV, tin-117m and contaminants cross section measurements have been investigated at the ARRONAX cyclotron using natural cadmium targets and alpha particles up to 65 MeV. From these results, a method has been defined to extract the tin-117m production cross section values from a Cd-116 enriched target. Thick target yield, radionuclidic purity and specific activity have been studied using experimental data and the TALYS 1.6 code values. This latter step was necessary for the determination of the number of stable and long-lived isotopes produced during the irradiation. Using the isotopic composition of commercialized enriched Cd-116 target, the maximum specific activity reached 40.3 kCi/g at 39.5 MeV. From our work, the irradiation parameters can be determined as a function of the required purity of the final product from 20.8 MeV up to 65 MeV.

5. Acknowledgments

Authors would like to thanks all the GIP ARRONAX team for their contribution. The ARRONAX cyclotron is a project promoted by the Regional Council of Pays de la Loire financed by local authorities, the French government and the European Union. This work has been, in part, supported by a grant from the French National Agency for Research called "Investissements d'Avenir", Equipex Arronax-Plus n° ANR-11-EQPX-0004 and Labex n° ANR-11-LABX-0018-01.

radionuclide	$T_{1/2}$	E_{γ} (keV)	I_{γ} (%)	Contributing reaction(s)	Threshold (MeV)
Sn-117m	13.60 (4) d	156.02	2.113 (6)	Cd-114(α ,n)	5.45
		158.562	86	Cd-116(α ,3n)	20.80
Sn-110	4.154 (4) h	280.459	97.06 (8)	Cd-108(α ,2n)	17.76
				Cd-110(α ,4n)	35.62
				Cd-111(α ,5n)	42.83
				Cd-112(α ,6n)	54.52
				Cd-113(α ,7n)	63.47
Sn-113g	115.09 (4) d	391.690	64	Cd-110(α ,n)	7.95
				Cd-111(α ,2n)	15.17
				Cd-112(α ,3n)	24.90
				Cd-113(α ,4n)	31.66
				Cd-114(α ,5n)	41.01
				Cd-116(α ,7n)	56.34
Cd-115g	53.46 (10) h	527.9	27.45 (18)	Cd-116(α , α +n)	9.00
				Cd-114(α ,2p+n)	22.93
				Cd-116(α ,2p+3n)	38.27

Table 6: Physical characteristics of tin and cadmium radionuclides (QCALC, 1995, Kinsey et al., 1996, Ekström and Firestone, 2004)

radionuclide	$T_{1/2}$	E_{γ} (keV)	I_{γ} (%)	Contributing reaction(s)	Threshold (MeV)
In-109	4.2 (1) h	203.5	74	Cd-106(α ,p) Cd-110(α ,2n+p) Cd-110(α ,4n+p) Cd-111(α ,5n+p) Cd-112(α ,6n+p)	5.72 24.65 42.50 49.72 59.43
In-110	4.9 (1) h	641.68 707.4 937.493 997.256	25.9 (6) 29.5 (10) 68.4 (14) 10.52 (20)	Cd-108(α ,n+p) Cd-110(α ,3n+p) Cd-111(α ,4n+p) Cd-112(α ,5n+p) Cd-113(α ,6n+p)	16.30 34.16 41.37 51.09 57.84
In-111	2.8047 (5) d	171.28 245.395	90 94	Cd-108(α ,p) Cd-110(α ,2n+p) Cd-111(α ,3n+p) Cd-112(α ,4n+p) Cd-113(α ,5n+p) Cd-114(α ,6n+p)	5.94 23.80 31.02 40.74 47.50 56.85
In-114m1	49.51 (1) d	190.29 558.456 725.298	15.56 (15) 3.24 (23) 3.24 (23)	Cd-111(α ,p) Cd-112(α ,n+p) Cd-113(α ,2n+p) Cd-114(α ,3n+p) Cd-116(α ,5n+p)	6.25 15.98 22.74 32.10 47.43

Table 7: Physical characteristics of indium radionuclides (QCALC, 1995, Kinsey et al., 1996, Ekström and Firestone, 2004)

Energy (MeV)	σ Sn-117m (mb)	σ Sn-113 (cum.) (mb)	σ Sn-110 (mb)	σ In-109 (mb)
65.01 \pm 0.68	5.44 \pm 0.70	218.91 \pm 28.25	78.29 \pm 9.97	44.74 \pm 7.31
55.13 \pm 0.93	10.82 \pm 1.21	214.40 \pm 24.94	63.90 \pm 7.23	8.99 \pm 1.63
48.92 \pm 1.08	17.58 \pm 2.02	212.50 \pm 25.01	23.68 \pm 2.75	8.67 \pm 1.37
45.86 \pm 1.16	24.16 \pm 3.29	224.67 \pm 32.06	10.32 \pm 1.38	8.21 \pm 1.34
42.10 \pm 1.25	40.93 \pm 4.63	216.31 \pm 25.30	2.89 \pm 0.34	6.03 \pm 0.71
39.51 \pm 1.37	59.07 \pm 6.66	220.67 \pm 28.33	3.63 \pm 0.44	5.14 \pm 0.73
35.43 \pm 1.52	81.84 \pm 7.74	209.97 \pm 21.38	6.71 \pm 0.70	2.07 \pm 0.34
32.24 \pm 1.61	76.89 \pm 9.88	180.53 \pm 25.70	7.80 \pm 1.03	1.51 \pm 0.26
29.25 \pm 1.76	49.29 \pm 6.15	148.41 \pm 19.00	7.48 \pm 0.98	3.38 \pm 0.52
25.26 \pm 1.93	19.28 \pm 2.43	183.31 \pm 23.10	4.99 \pm 0.64	11.97 \pm 1.54

Table 8: Production cross section values of Sn-110, Sn-113 and Sn-117m from the Cd-nat(α ,xn) reaction and In-109 from the Cd-nat(α ,x) reaction.

Energy (MeV)	σ In-110g (mb)	σ In-111 (mb)	σ In-114m (mb)	σ Cd-115g (mb)
65.01 \pm 0.68	88.23 \pm 13.14	271.38 \pm 34.00	64.18 \pm 8.32	5.59 \pm 0.71
55.13 \pm 0.93	44.62 \pm 6.04	233.57 \pm 25.90	69.40 \pm 8.34	4.80 \pm 0.60
48.92 \pm 1.08	11.44 \pm 1.59	197.33 \pm 22.34	43.78 \pm 6.17	3.77 \pm 0.43
45.86 \pm 1.16	3.83 \pm 0.61	169.51 \pm 21.64	33.47 \pm 4.59	3.00 \pm 0.45
42.10 \pm 1.25	1.53 \pm 0.61	116.65 \pm 13.19	23.80 \pm 2.99	2.05 \pm 0.27
39.51 \pm 1.37	1.78 \pm 0.27	106.31 \pm 11.94	24.99 \pm 3.15	1.95 \pm 0.27
35.43 \pm 1.52	2.03 \pm 0.29	49.91 \pm 4.73	22.63 \pm 2.37	2.15 \pm 0.25
32.24 \pm 1.61	2.20 \pm 0.35	17.11 \pm 2.20	16.87 \pm 2.28	0.92 \pm 0.13
29.25 \pm 1.76	1.56 \pm 0.26	2.77 \pm 0.35	9.51 \pm 1.46	
25.26 \pm 1.93	0.55 \pm 0.08	7.57 \pm 0.95	4.89 \pm 1.62	0.30 \pm 0.05

Table 9: Production cross section values of In-110g, In-111, In-114m and Cd-115g from the Cd-nat(α ,x) reaction.

6. References

- Adam Rebeles R., Hermanne A, Van den Winkel P., Tárkányi F., Takács S., and Darabanc L., 2008. Alpha induced reactions on ^{114}Cd and ^{116}Cd : An experimental study of excitation functions. *Nuclear Instruments and Methods in Physics Research Section B : Beam Interactions with Materials and Atoms*, 266, 4731-37.
- Atkins H.L., Mausner L.F., Srivastava S.C., Meinken G.E., Straub R.F., Cabahug C.I., Weber D.A., Wong. C.T.C., Sacker D.F., Madajewicz S., Park L., and Meek A.G., 1993. Biodistribution of $^{117m}\text{Sn}(4+)\text{DTPA}$ for palliative therapy of painful osseous metastases. *Radiobiology*, 186 (1), 279-83.
- Bishayee A., Rao D.V., Srivastava S.C., Bouchet L.G., Bolch W.E., and Howell R.W., 2000. Marrow-sparing effects of $^{117m}\text{Sn}(4+)\text{Diethylenetriaminepentaacetic acid}$ for radionuclide therapy of bone cancer. *Int. J. Nucl. Med. Biol.*, 41 (12), 2043-50.
- Clear Vascular Inc. Clinical stage company. <http://www.clearvascular.com/>, 2015.
- Collins C., Eary J.F., Donaldson G., Vernon C., Bush N.E., Petersdorf S., Livingston R.B., Gordon E.E., Chapman C.R., and Appelbaum F.R., 1993. Samarium-153-EDTMP in hormone refractory prostate cancer : a phase I/II trial. *J. Nucl. Med.*, 34 (7), 1031-6.
- De Klerk I.M.H., Zonnenberg B.A., van het Schip A.D., van Dijk A., Quirijnen I.M.S.P., Hoekstra A., and van Rijk P.P., 1997. Treatment of metastatic bone pain using the bone seeking radiopharmaceutical Re-186-HEDP . *Anticancer Res.* 17, 1773-77.
- Demetriou P., Grama C., and Goriely S, 2002. Improved global alpha-optical model potentials at low energies. *Nucl. Phys. A*, 707 (1-2), 253-76.
- Duchemin C., Guertin A., Haddad F., Michel N. and Métivier V., 2015. Production of medical isotopes from a thorium target irradiated by light charged particles up to 70 MeV, *Phys. Med. Biol.* 60, 931-946.
- Ekström, L.F., and Firestone, R.B., 2004. Information extracted from the table of Radioactive Isotopes, version 2.1.
- Ermolaev S.V., Zhuikov B.L., Kokhanyuk V.M., and Srivastava S.C., 2007. Production yields of ^{117m}Sn from natural antimony target in proton energy range 145 - 35 MeV. *Journal of Labelled Compounds and Radiopharmaceuticals*, 50, 611-2.
- FitzPeaks Gamma Analysis and Calibration Software version 3.66, produced by JF Computing Services (UK), based on methods presented in

Nucl.Instrum. and Methods (1981) 190, 89-99, describing the program SAMPO80 of the Helsinki University of Technology, Finland.

Gadioli E. and Hodgson P.E., Pre-equilibrium nuclear reactions, Oxford Univ. Press (1992), 530 pages, ISBN 9780198517344..

Goodfellow website. Tous les matriaux pour la recherche, l'industrie et la production. www.goodfellow.com, 2015.10.29.

Goriely S., Hilaire S. and Koning A.J., 2008. Improved microscopic nuclear level densities within the HFB plus combinatorial method, Phys. Rev. C 78 (6), 064307, 14.

Haddad, F., Ferrer, L., Guertin, A., Carlier, T., Michel, N., Barbet, J., Chatal, J.F., 2008. Arronax a high-energy and high-intensity cyclotron for nuclear medicine, Eur. J. Nucl. Med. Mol. Imaging 35, 1377-1387.

Hermanne A., Daraban L., Adam Rebeles R., Ignatyuk A., Tárkányi F., and Takács S, 2010. Alpha induced reactions on natCd up to 38.5 MeV : Experimental and theoretical studies of the excitation functions. Nuclear Instruments and Methods in Physics Research B, 268 (9), 1376-91.

IAEA, 2009. Cyclotron produced radionuclides : physical characteristics and production methods. Vienna. Technical Reports Series No. 468.

IAEA-NDS, 2015. LiveChart of nuclides. Available on www-nds.iaea.org.

International Atomic Energy Agency, 2008. Cyclotron produced radionuclides : Principles and practice. Technical reports series, 465.

Joshi D.P., Seery W.H., Goldberg L.G. and Goldman L., 1965. Evaluation of ³²P-phosphorus for intractable pain secondary to prostatic carcinoma metastasis. J. Am. Med. Assoc., 193, 7, 621-3.

Koning, A.J., Rochman, D., 2012. Modern nuclear data evaluation with the TALYS code system, Nucl. Data Sheets 113, 2841. TALYS 1.6 version available on <http://www.talys.eu/>.

Lafont A., 2003. Basic aspects of plaque vulnerability. Heart., 89 (10), 1262-7.

Lewis S.S, Cox G.M. and Stout J.E., 2014. Clinical Utility of Indium 111Labeled White Blood Cell Scintigraphy for Evaluation of Suspected Infection. Open Forum Infect Dis, 1 (2): doi: 10.1093/ofid/ofu089.

Maxon H.R., Schroder L.E., Hertzberg V.S., Thomas S.R., Englaro E.E., Samaratunga R., Smith H., Moulton J.S., Williams C.C., Ehrhardt G.J., and Schneider H.I., 1991. Rhenium-186(Sn)HEDP for treatment of painful osseous metastases : results of a double-blind crossover comparison with placebo. J. Nucl. Med., 32 (10), 1877-81.

Montgomery D.M. and Porile N.T., 1969. Reactions of ^{116}Cd with intermediate energy ^3He and ^4He ions. *Nuclear Physics A*, 130 (1), 65-76.

Kinsey R.R. et al., The NUDAT/PCNUDAT Program for Nuclear Data, paper submitted to the 9th International Symposium of Capture Gamma-Ray Spectroscopy and Related Topics, Budapest, Hungary, October 1996. Data extracted from the NUDAT database, version 2.6.

QCALC, 1995. Data produced by the code QCALC, written by T.W. Burrows, National Nuclear Data Center, Brookhaven National Laboratory, and based on the Audi-Wapstra Atomic Mass Tables, G. Audi and A.H. Wapstra, The 1995 Update to the Atomic Mass Evaluation., *Nucl. Phys. A* 595, 409 (1995).

Oster Z.H, Som P., and Srivastava S.C. et al., 1995. The development and in-vivo behavior of tin containing radiopharmaceuticals II. Autoradiographic and scintigraphic studies in normal animals and in animal models of disease. *Int. J. Nucl. Med. Biol.*, 12 (3), 175-84.

Porter A., McEwan A.J.B., Powe J.E., Reid R., McGowan D.G., Lukka H., Sathyanarayana J.R., Yakemchuk V.N., Thomas G.M., Erlich L.E., Crook J., Gulenchyn K.Y., Hong K.E., Wesolowski C., and Yardley J., 1993. Results of a randomized phase III trial to evaluate the efficacy of strontium-89 adjuvant to local field external beam irradiation in the management of endocrine resistant metastatic prostate cancer. *J. Radiat. Oncol. Biol. Phys.*, 25 (5), 805-13.

Qaim S.M. and Döhler H., 1984. Production of carrier-free $^{117\text{m}}\text{Sn}$. *Int. J. Appl. Radiat. Isot.*, 35 (7), 645-50.

Resche I., Chatal J-F., Pecking A., Ell P., Duchesne G., Rubens R., Fogelman I., Houston S., Fauser A., Fischer M., and Wilkins D., 1997. A dose-controlled study of ^{153}Sm -ethylenediaminetetramethylenephosphonate (EDTMP) in the treatment of patients with painful bone metastases. *Eur. J. Cancer*, 33 (10), 1583-91.

Russian Academy of Sciences. Institute for nuclear research.<http://www.inr.ac.ru/>, 2015.05.29.

Srivastava S.C., Meinken G.E., Richards P., Som P., Oster Z.H., Atkins H.L., Brill A.B., Knapp F.F. Jr., and Butler T.A., 1985. The development and in vivo behavior of tin containing radiopharmaceuticals I. chemistry, preparation, and biodistribution in small animals. *Int. J. Nucl. Med. Biol.*, 1 (3), 175-84.

Srivastava S.C., Atkins H.L., and Krishnamurthy G.T. et al., 1998. Treatment of metastatic bone pain with tin- $^{117\text{m}}$ stannic DTPA : A phase I/II

clinical study. *Clin. Cancer Res.*, 4 (1), 61-8.

Srivastava S.C., 2014. Enabling simultaneous imaging and treatment with the theragnostic radionuclide tin-117m. *Nucl. Med. Biol.* 41 (7), 640.

Stevenson N.R., George G.St., Simón J., Srivastava S.C., Mueller D.W., Gonzales G.R., Rogers J.A., Frank R.K., Horn I.M. 2015. Methods of producing high specific activity Sn-117m with commercial cyclotrons. *J. Radioanal. Nucl. Chem.* 305 (1), 99-108.

Takács S., Takács M.P., Hermanne A., Tárkányi F., and Adam Rebeles R. 2013. Cross sections of proton induced reactions on natSb. *Nuclear Instruments and Methods in Physics Research Section B : Beam Interactions with Materials and Atoms*, 297, 44-57.

Tárkányi, F., Takács, S., Gul, K., Hermanne, A., Mustafa, M.G., Nortier, M., Oblozinsky, P., Qaim, S.M., Scholten, B., Shubin, Yu.N., Youxiang, Z., 2001. Beam monitor reactions, in *Charged Particle Cross Section Database for Medical Radioisotope Production: Diagnostic Radioisotopes and Monitor Reactions*; IAEA-TECDOC-1211, pages 49-152, IAEA, Vienna. Database available on <https://www-nds.iaea.org/medportal/>, update may 2013.

Trace Sciences International Inc., 2015. www.tracesciences.com.

Yano Y., Chu P., and Anger H.O., 1973. Tin-117m : Production, chemistry and evaluation as a bone-scanning agent. *International Journal of Applied Radiation and Isotopes*, 24 (6), 319-25.

Ziegler, J.F., Ziegler, M.D. and Biersack, J.P., 2010. SRIM The stopping and range of ions in matter, *Nucl. Instrum. Methods Phys. Res., Sect. B* 268 (11-12), 1818-23.